Inorg. Chem. **2004**, *43*, 8263–8271

Voltammetric Reduction of α- and γ*-$[S_2W_{18}O_{62}]^{4-}$ and α-, β-, and γ-$[SiW_{12}O_{40}]^{4-}$: Isomeric Dependence of Reversible Potentials of Polyoxometalate Anions Using Data Obtained by Novel Dissolution and Conventional Solution-Phase Processes

Jie Zhang and Alan M. Bond*

School of Chemistry, Monash University, Clayton, Victoria 3800, Australia

Peter J. S. Richardt and Anthony G. Wedd*

School of Chemistry, University of Melbourne, Parkville, Victoria 3052, Australia

Received July 19, 2004

Comparative studies on the voltammetric reduction of the α and γ* isomers of Dawson $[S_2W_{18}O_{62}]^{4-}$ and α, β, and γ forms of Keggin $[SiW_{12}O_{40}]^{4-}$ polyoxometalate anions have been undertaken. For the six reversible one-electron $[S_2W_{18}O_{62}]^{4-/5-/6-/7-/8-/9-/10-}$ processes in acetonitrile, reversible potentials ($E^{0'}$) were found to be independent of isomeric form within experimental error (±5 mV). However, because both the α and γ* isomers of $[Bu_4N]_4[S_2W_{18}O_{62}]$ are insoluble in water, solid-state voltammetric studies with microcrystals adhered to electrode surfaces in contact with aqueous Et_4NCl and Bu_4NCl electrolyte media were also possible. Although no isomeric distinction was again detected in the solid-state studies, it was found that reduction of adhered solid by four or more electron equivalents led to rapid dissolution. When Et_4NCl was the electrolyte, this dissolution process coupled with potential cycling experiments enabled conventional solution-phase data to be obtained in water for the analogous six one-electron reduction steps previously detected in acetonitrile. A strong medium effect attributed to Lewis acidity effects was apparent upon comparison with $E^{0'}$ data obtained in water and acetonitrile. In contrast, with the $[SiW_{12}O_{40}]^{4-}$ system, $E^{0'}$ values for the $[SiW_{12}O_{40}]^{4-/5-/6-/7-}$ processes in acetonitrile exhibited a larger (about 70 mV) dependence on isomeric form, and the isomerization step, $[\gamma\text{-}SiW_{12}O_{40}]^{6-} \rightarrow [\alpha\text{-}SiW_{12}O_{40}]^{6-}$, was detected on the voltammetric time scale. The influence of isomeric form on reversible potential data is considered in terms of structural and charge density differences exhibited in the $[S_2W_{18}O_{62}]^{4-}$ and $[SiW_{12}O_{40}]^{4-}$ systems studied in this paper and published data available on the α, β, γ, and γ* isomers of $[As_2W_{18}O_{62}]^{6-}$ and $[P_2W_{18}O_{62}]^{6-}$ Dawson anions and Keggin systems.

Introduction

Polyoxometalate anions exhibit a wide range of structural, redox, and catalytic properties. As a consequence, their chemistry has been investigated intensively for reasons of both fundamental and applied significance.[1] Electrochemical methods have been used extensively to establish the reversible potentials associated with the rich electrochemistry of polyoxometalates and also to achieve the directed synthesis and characterization of their reduced forms.[2] The present work considers electrochemical properties of isomeric forms of two classic polyoxometalate structures. The α isomer of a Keggin anion $[XM_{12}O_{40}]^{n-}$ consists of four M_3 caps of edge-sharing MO_6 octahedra giving rise to a structure of highest point symmetry (T_d; structure I, Chart 1).[1a] Structural representations of the four possible other isomers, β (C_{3v}), γ (C_{2v}), δ (C_{3v}), and ε (T_d), available in refs 1a,f, are derived from the α form by systematic rotation of the M_3 caps by 60°. The α isomer of the closely related Dawson anions

* To whom correspondence should be addressed. E-mail: alan.bond@sci.monash.edu.au (A.M.B.), agw@unimelb.edu.au (A.G.W.).

(1) (a) Pope, M. T. *Heteropoly and Isopoly Oxometalates*; Springer-Verlag: Berlin, 1983. (b) Pope, M. T.; Müller, A. *Angew. Chem., Int. Ed. Engl.* **1991**, *30*, 34. (c) Hill, C. L.; Prosser-McCartha, C. M. Coord. *Chem. Rev.* **1995**, *143*, 407. (d) *Chem. Rev.* **1998**, *98*, 1−387. (e) Hiskia, A.; Mylonas, A.; Papaconstantinou, E. *Chem. Soc. Rev.* **2001**, *30*, 62. (f) Pope, M. T. In *Comprehensive Coordination Chemistry II*; McCleverty, J. A., Meyer, T. J., Eds.; Elsevier: Amsterdam, 2004; Vol. 4, p 635. (g) Hill, C. L. In *Comprehensive Coordination Chemistry II*; McCleverty, J. A., Meyer, T. J., Eds.; Elsevier: Amsterdam, 2004; Vol. 4, p 679.

(2) Sadakane, M.; Steckhan, E. *Chem. Rev.* **1998**, *98*, 219.

10.1021/ic049043x CCC: $27.50
Published on Web 11/19/2004

Chart 1. Polyhedral Representations of α Isomers of Keggin (structure I) and Dawson (structure II) Anions

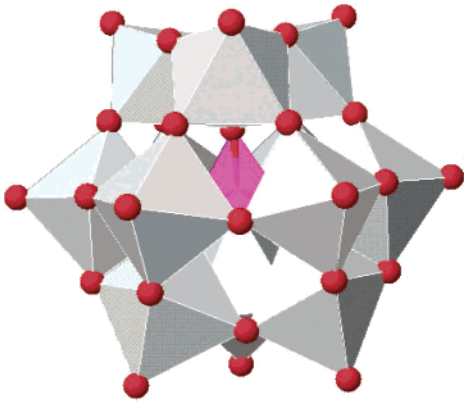

I

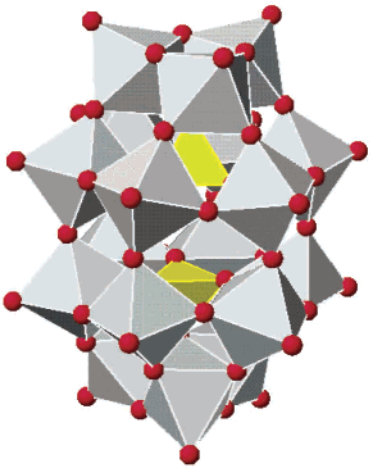

II

$[X_2M_{18}O_{62}]^{n-}$ also represents the structure of highest point symmetry (D_{3h}; structure II, Chart 1). In this case, a total of five other possible isomers (α*, β, β*, γ, and γ*) are related by 60° rotations of the M_3 caps and/or M_6 belts. In particular, the γ* isomer (D_{3h}), which is of interest in this study, is derived from the α form by formal rotation of one cap and one belt.[1f,3,4]

Synthesis and structural characterization of $[Bu_4N]_4[\gamma^*\text{-}S_2W_{18}O_{62}]$ has been described.[3,5] Under voltammetric conditions, this anion has been reported to exhibit four reversible one-electron processes in acetonitrile (0.1 M Bu_4NClO_4).[3] Interestingly, the one-electron-reduced anion $[\alpha\text{-}S_2W_{18}O_{62}]^{5-}$ rather than the γ* isomer was isolated after controlled potential electrolysis.[5] Subsequently, $[\alpha\text{-}S_2W_{18}O_{62}]^{4-}$ was isolated and structurally characterized.[6] Intriguingly, the four reversible solution-phase potentials reported[3,5,6] for the α and γ* forms in CH_3CN (0.1 M Bu_4NClO_4) are experimentally indistinguishable. The only directly comparable Dawson system for which voltammetric data are available is the $[As_2W_{18}O_{62}]^{6-/7-}$ process.[4] In this case, the cited differences in reversible potentials are 30 mV. In contrast, limited data available on the α, β, and γ isomers of the Keggin $[SiW_{12}O_{40}]^{4-}$ polyoxometalate anions imply that reversible potentials of this series of isomers differ significantly[7−10] and much more than is the case with their larger and more highly charged α-, β-, and γ-$[As_2W_{18}O_{62}]^{6-}$ and $[P_2W_{18}O_{62}]^{6-}$ Dawson analogues.[4] Accurate reversible potential data on the $[S_2W_{18}O_{62}]^{4-}$ and $[SiW_{12}O_{40}]^{4-}$ systems obtained in the present studies therefore enable the influence of structure and charge distribution on the reversible potential of the different classes of polyoxometalate to be examined in a systematic manner.

In view of the similarity in the solution-phase voltammetry of the α and γ* isomeric forms in acetonitrile, studies were undertaken on solid $[Bu_4N]_4[S_2W_{18}O_{62}]$ adhered to an electrode surface in contact with aqueous electrolyte media[11−13] in order to establish whether the nature of the phase is important. Intriguingly, although the potentials for reduction of solid α and γ* remain indistinguishable, after a 4-electron reduction of solid $[Bu_4N]_4[S_2W_{18}O_{62}]$ in contact with the aqueous electrolyte media, rapid dissolution of solid occurs, enabling the potentials of the six one-electron $[S_2W_{18}O_{62}]^{4-/5-/6-/7-/8-/9-/10-}$ processes to be established and compared with data obtained in acetonitrile. Consequently, exploitation of this novel dissolution reaction confirms that reduction potentials for both the solid and solution-phase species are indistinguishable, but enables the medium dependence of the reversible potential to be detected and considered in terms of Lewis acidity of the solvent.

Experimental Section

Materials. The α isomer of $[Bu_4N]_4[S_2W_{18}O_{62}]$ was synthesized by the method of Himeno.[6] The procedure involves heating a reaction mixture of $Na_2WO_4{\cdot}2H_2O$, H_2SO_4, CH_3CN, and H_2O at 70 °C for 14 days. On the other hand, the procedure reported for the synthesis of the γ* isomer involves heating at reflux overnight only and leads to a mixture of $[Bu_4N]^+$ salts of $[W_6O_{19}]^{2-}$, $[\alpha\text{-}S_2W_{18}O_{62}]^{4-}$, and $[\gamma^*\text{-}S_2W_{18}O_{62}]^{4-}$.[3] Fractional crystallization from hot CH_3CN provides analytically pure material, but this material is a mixture of crystals of $[Bu_4N]_4[\alpha\text{-}S_2W_{18}O_{62}]$ and $[Bu_4N]_4[\gamma^*\text{-}S_2W_{18}O_{62}]$ containing solvent of crystallization. The crystals lose solvent rapidly upon exposure to air. Samples with a high proportion of crystals of the γ* form (≥90% isomeric purity) were obtained by manual crystal picking and are referred to as the γ* form in the text. The α, β, and γ isomers of $[Bu_4N]_4[SiW_{12}O_{40}]$ were synthesized as described in the literature.[7,8]

Bu_4NCl (98%, Sigma-Aldrich), 1-butyl-3-methylimidazolium chloride (≥99%, Sigma-Aldrich), and Et_4NCl (analytical grade,

(3) Richardt, P. J. S.; Gable, R. W.; Bond, A. M.; Wedd, A. G. *Inorg. Chem.* **2001**, *40*, 703 and references therein.
(4) Contant, R.; Thouvenot, R. *Inorg. Chim. Acta* **1993**, *212*, 41.
(5) Richardt, P. J. S.; White, J. M.; Tregloan, P. A.; Bond, A. M.; Wedd, A. G. *Can. J. Chem.* **2001**, *79*, 613.
(6) Himeno, S.; Tatewaki, H.; Hashimoto, M. *Bull. Chem. Soc. Jpn.* **2001**, *74*, 1623.
(7) Tézé, A.; Hervé, G. *Inorg. Synth.* **1990**, *27*, 85.
(8) Rocchiccioli-Deltcheff, C.; Fournier, M.; Franck, R.; Thouvenot, R. *Inorg. Chem.* **1983**, *22*, 207.
(9) Tézé, A.; Canny, J.; Gurban, L.; Thouvenot, R.; Hervé, G. *Inorg. Chem.* **1996**, *35*, 1001.
(10) Richardt, P. J. S. Ph.D. Thesis, Melbourne University, Melbourne, Australia, 2000.
(11) Scholz, F.; Lange, B. *Trends Anal. Chem.* **1992**, *11*, 359.
(12) Bond, A. M. *Broadening Electrochemical Horizons: Principles and Illustration of Voltammetric and Related Techniques*; Oxford University Press: Oxford, U.K., 2002.
(13) Bond, A. M.; Cooper, J. B.; Marken, F.; Way, D. M. *J. Electroanal. Chem.* **1995**, *396*, 407.

BDH) salts were used to prepare aqueous electrolytes in triply distilled water. CH_3CN (BDH, analytical grade) was dried over basic alumina before use. Bu_4NPF_6 used as the electrolyte for voltammetric studies in CH_3CN was purchased from GFS and recrystallized twice from hot EtOH.[14] Bu_4NClO_4 was prepared by addition of Bu_4NOH to aqueous $HClO_4$. All other chemicals were of analytical grade purity and were used as supplied by the manufacturers.

Electrochemical Instrumentation and Procedures. Cyclic voltammetric measurements were undertaken with BAS 100B (Bioanalytical Systems, IN) or CS-1090 (Cypress Systems, KS) electrochemical workstations. Glassy carbon (GC) or gold disk electrodes (d = 1 or 3 mm) were employed as the working electrode, and prior to use, these were polished with an Al_2O_3 slurry (0.3 μm; Buehler), washed successively with water and acetone, and then dried with tissue paper. Pt wire was used as the counter electrode. For measurements in aqueous electrolyte media, a Ag/AgCl (3 M NaCl) reference was used. For the measurements in CH_3CN, either a Ag/Ag^+ (10^{-3} M $AgNO_3$ in CH_3CN) reference electrode or a Pt wire quasi-reference electrode was used. The potential scale for studies in CH_3CN was calibrated against the Fc^+/Fc scale by employing the voltammetric oxidation of 1×10^{-3} M ferrocene (Fc) as an internal reference.[15]

For the electrochemical quartz crystal microbalance (EQCM) measurements,[16] a PM-700 series plating monitor (Maxtek, CA) was used with 9-MHz gold-coated AT-cut quartz crystals (d = 1.32 cm, electrode area = 1.37 cm^2) as the working electrode. The monitor was interfaced to an Autolab electrochemical work station (Eco Chime, Utrecht, The Netherlands) for simultaneous measurement of voltammetric and mass change data. The reference and counter electrodes were the same as those used in the aqueous media voltammetric measurements. The EQCM instrument was calibrated via the electrodeposition of copper from a 0.010 M $CuSO_4$ aqueous solution (supporting electrolytes, 2 M KNO_3 and 0.010 M HNO_3).[17]

The procedure employed for mechanical attachment of microcrystalline solid onto the working electrode surface has been described in detail.[18] In brief, a few milligrams of $[Bu_4N]_4[S_2W_{18}O_{62}]$ solid was placed on sample weighing paper. The working electrode was then pressed onto the substrate and rubbed over the surface so that arrays of microcrystals adhered to the electrode surface.

All experiments were conducted at ambient temperature of 20 ± 1 °C. Prior to electrochemical experiments, solutions were degassed for at least 10 min with high-purity nitrogen in order to remove oxygen.

Results and Discussion

Part A. Electrochemical Studies with α and γ* Isomers of $[S_2W_{18}O_{62}]^{4-}$. Cyclic Voltammetric Studies in CH_3CN (0.1 M Bu_4NPF_6). In acetonitrile, experimentally indistinguishable voltammograms are obtained at a GC macrodisc (d = 1 mm) working electrode for the α (Figure 1) and γ* isomers. In either case, six well-defined reversible one-electron-transfer steps (labeled 1−6 in Figure 1) are detected. The reversible potentials for the six couples $[S_2W_{18}O_{62}]^{n-/(n+1)-}$ (n = 4−9) [$E^{0'} = (E_p^{red} + E_p^{ox})/2$] are estimated with an uncertainty of ±5 mV as −0.240, −0.615, −1.180, −1.565, −2.020, and −2.320 V versus Fc^+/Fc over the scan rate range of 10−1000 mV s^{-1}. Peak-to-peak separations of $\Delta E_p \approx 80$ mV at a scan rate of 200 mV s^{-1} are observed, a value comparable to those found for the known reversible one-electron Fc^+/Fc reference system.[14] The deviation from the theoretically predicted value of 56 mV at 20 °C is attributed to a low level of uncompensated resistance.[19] Chemical reversibility is indicated for all processes as each peak current ratio $|I_p^{red}:I_p^{ox}| \approx 1.0$. Table 1 summarizes voltammetric data obtained in CH_3CN media. The additional feature found in the present study relative to data reported in refs 3, 5, and 6 is the detection of processes 5 and 6. This is attributed to the extended negative potential range made available by drying the solvent over basic alumina prior to use in voltammetric experiments.

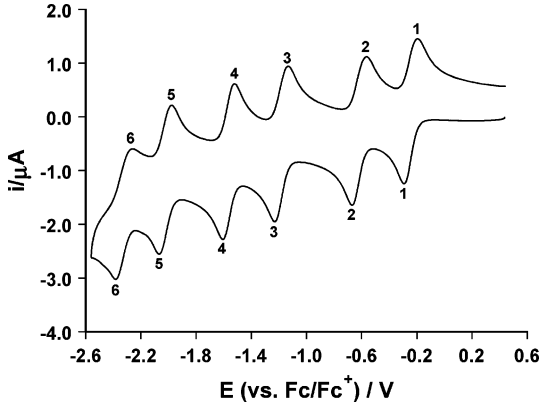

Figure 1. Cyclic voltammograms (υ = 200 mV s^{-1}) for $[\alpha\text{-}S_2W_{18}O_{62}]^{4-}$ (5.0×10^{-4} M) in CH_3CN (0.1 M Bu_4NPF_6) at a GC macrodisc electrode (d = 1 mm).

Cyclic Voltammetric Studies of Solids Adhered to a GC Working Electrode in Contact with Aqueous Electrolyte Media. Voltammetric studies of water-insoluble $[Bu_4N]_4[S_2W_{18}O_{62}]$ adhered to an electrode surface in contact with aqueous media were undertaken with either Et_4NCl (change of cation) or Bu_4NCl (common cation) as the electrolyte in order to ascertain whether the change to the solid state will enable the voltammetry of α- and γ*-$[S_2W_{18}O_{62}]^{4-}$ to be distinguished and also to determine whether the identity of the electrolyte cation is significant.

(i) Et_4NCl as the Aqueous Electrolyte. Solid $[Bu_4N]_4[\alpha\text{-}S_2W_{18}O_{62}]$ adhered to a GC electrode (d = 1 mm) was placed in contact with 0.1 M Et_4NCl aqueous electrolyte solution. On the first potential sweep, two chemically nonreversible processes are observed under the conditions of Figure 2 (peak a, −0.80; peak b, −1.16 V versus Ag/AgCl). However, on repetitive potential cycling, these two reduction processes are replaced by a series of reversible one-electron processes (labeled 1−6 in Figure 2a) that have

(14) Sawyer, D. T.; Sobkowiak, A.; Roberts, J. L., Jr. *Electrochemistry for Chemists*, 2nd ed.; Wiley: New York, 1995.
(15) Gritzner, G.; Kuta, J. *Pure Appl. Chem.* **1984**, *45*, 461.
(16) For reviews, see, for example: (a) Ward, M. D. In *Physical Electrochemistry, Principles, Methods, and Applications*; Rubinstein I., Ed.; Marcel Dekker: New York, p 293. (b) Ward, M. D.; Buttry, D. A. *Science* **1990**, *249*, 1000. (c) Buttry, D. A.; Ward, M. D. *Chem. Rev.* **1992**, *92*, 1355.
(17) (a) Deakin, M. R.; Melroy, O. *J. Electroanal. Chem.* **1988**, *239*, 321. (b) Bond, A. M.; Miao, W.; Raston, C. L. *J. Phys. Chem. B* **2000**, *104*, 2320.
(18) Zhang, J.; Bond, A. M. *Anal. Chem.* **2003**, *75*, 6938.
(19) Bard, A. J.; Faulkner, L. R. *Electrochemical Methods, Fundamentals and Applications*, 2nd ed.; Wiley: New York, 2001.

Table 1. Reversible Potentials[a] (vs Fc^+/Fc) Obtained for the Reduction of the α and γ* Forms of $[S_2W_{18}O_{62}]^{4-}$ in CH_3CN (100%), CH_3CN/H_2O (95:5 v/v), and Aqueous Electrolyte Media

isomeric form	solvent	electrolyte (0.1 M)	working electrode	$E^{0'}$/V process 1	process 2	process 3	process 4	process 5	process 6
α and γ*	CH_3CN[b]	Bu_4NPF_6	GC	−0.24	−0.62	−1.18	−1.57	−2.02	−2.32
	H_2O[c]	Et_4NCl	GC	0.02	−0.20	−0.64	−0.89	−1.08	−1.20
			Au	0.02	−0.19	−0.63	−0.90		
γ*	CH_3CN[d]	Bu_4NClO_4	GC	−0.24	−0.62	−1.18	−1.57		
	CH_3CN/H_2O (95:5)[d]	Bu_4NClO_4	GC	−0.23	−0.59	−1.12	−1.42		
α	CH_3CN[e]	Bu_4NClO_4	GC	−0.27	−0.65	−1.21	−1.60		

[a] Calculated as $(E_p^{red} + E_p^{ox})/2$ from cyclic voltammograms. [b] Experimental conditions are summarized in the caption to Figure 1. [c] Experimental conditions are summarized in the caption to Figure 2 (GC) and Figure S3 (Au). The measured $E^{0'}$ value (vs Ag/AgCl) is converted (small temperature difference neglected) to the Fc^+/Fc scale using the Ag/AgCl and Fc/Fc^+ standard potentials in aqueous media of 0.212[14] and 0.44[33] vs NHE, respectively, at 25 °C. [d] Data are from ref 3. [e] Data are from ref 6 and are corrected to the Fc/Fc^+ scale using the potential difference of −0.089 V at 25 °C.[34] The constant difference of 0.03 V for all processes in refs 3 and 6 might represent an error associated with junction potentials of unknown magnitude.

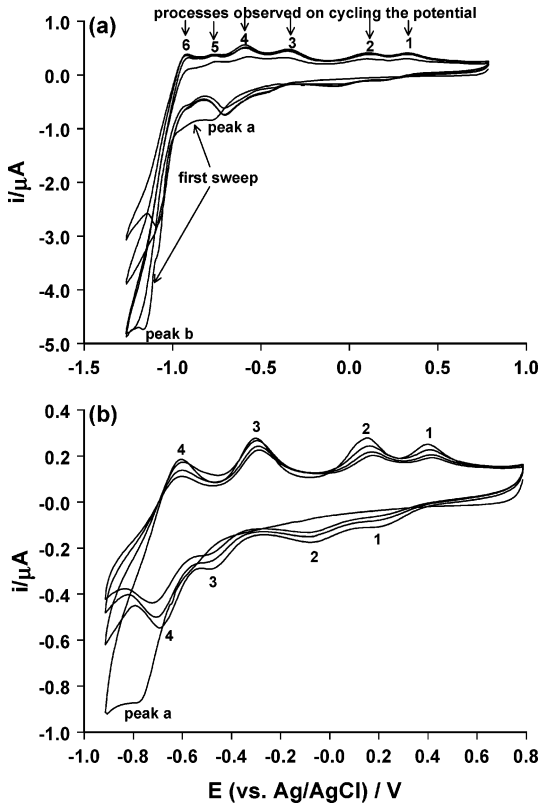

Figure 2. Cyclic voltammograms ($v = 100$ mV s^{-1}) for solid $[Bu_4N]_4[\alpha\text{-}S_2W_{18}O_{62}]$ adhered to a GC electrode ($d = 1$ mm) in contact with aqueous electrolyte (0.1 M Et_4NCl). The potential was cycled (a) between 0.8 and −1.35 V and (b) between 0.8 and −0.9 V.

many of the characteristics detected for $[Bu_4N]_4[S_2W_{18}O_{62}]$ dissolved in CH_3CN (0.1 M Bu_4NPF_6) (Figure 1). Switching the potential immediately after peak a appears to lead to rapid dissolution of the four-electron-reduced anion $[S_2W_{18}O_{62}]^{8-}$ (Figure 2b) and the concomitant observation of four chemically reversible one-electron solution processes. If switching is delayed until after peak b, six reversible one-electron processes are observed (Figure 2a). The estimated reversible potentials obtained in aqueous media are summarized in Table 1.

Blue material, detected visually on and near to the electrode surface during the course of voltammetric experiments, is consistent with the formation of reduced compound.[5] If a switching potential less negative than −0.5 V vs Ag/AgCl was employed, no voltammetric responses were detected in the second and subsequent cycles. All of the data lead to the conclusion that reduction of solid at peak a generates dissolved $[S_2W_{18}O_{62}]^{8-}$ (eq 1), which is then followed by the reaction sequence summarized in eqs 2−5

$$[S_2W_{18}O_{62}]^{4-}(s) + 4e^- \rightarrow [S_2W_{18}O_{62}]^{8-}(aq) \quad (1)$$

$$[S_2W_{18}O_{62}]^{8-}(aq) \rightleftarrows [S_2W_{18}O_{62}]^{7-}(aq) + e^- \quad \text{process 4} \quad (2)$$

$$[S_2W_{18}O_{62}]^{7-}(aq) \rightleftarrows [S_2W_{18}O_{62}]^{6-}(aq) + e^- \quad \text{process 3} \quad (3)$$

$$[S_2W_{18}O_{62}]^{6-}(aq) \rightleftarrows [S_2W_{18}O_{62}]^{5-}(aq) + e^- \quad \text{process 2} \quad (4)$$

$$[S_2W_{18}O_{62}]^{5-}(aq) \rightleftarrows [S_2W_{18}O_{62}]^{4-}(aq) + e^- \quad \text{process 1} \quad (5)$$

Apparently, dissolved $[S_2W_{18}O_{62}]^{8-}(aq)$ diffuses into the bulk solution, and reprecipitation does not occur during the course of oxidation processes 4 to 1 on the voltammetric time scale employed in Figure 2. Switching at more negative potentials than peak b gives rise to more highly reduced species and, hence, additional solution-based processes (eqs 6 and 7)

$$[S_2W_{18}O_{62}]^{10-}(aq) \rightleftarrows [S_2W_{18}O_{62}]^{9-}(aq) + e^- \quad \text{process 6} \quad (6)$$

$$[S_2W_{18}O_{62}]^{9-}(aq) \rightleftarrows [S_2W_{18}O_{62}]^{8-}(aq) + e^- \quad \text{process 5} \quad (7)$$

Figure 3 shows cyclic voltammograms obtained as a function of scan rate over the potential range from 0.8 to −1.35 V. The behavior is consistent with transfer of reduced anions from the solid state to the solution phase followed by diffusion into the bulk aqueous electrolyte solution without reprecipitation. At the lowest scan rate examined (20 mV s^{-1}), little evidence of solution processes is apparent (Figure 3a). The currents associated with peaks a and b decrease as the potential is cycled, presumably because of transport of electroactive material away from the electrode surface. However, when the scan rate is increased to 100 mV s^{-1} (Figure 3b), significant currents are detected for the solution voltammetric responses, consistent with the shorter time available for product diffusion. At the highest scan rate examined (1000 mV s^{-1}), solution processes 1−6 were enhanced on repetitive cycling of the potential (Figure 3c).

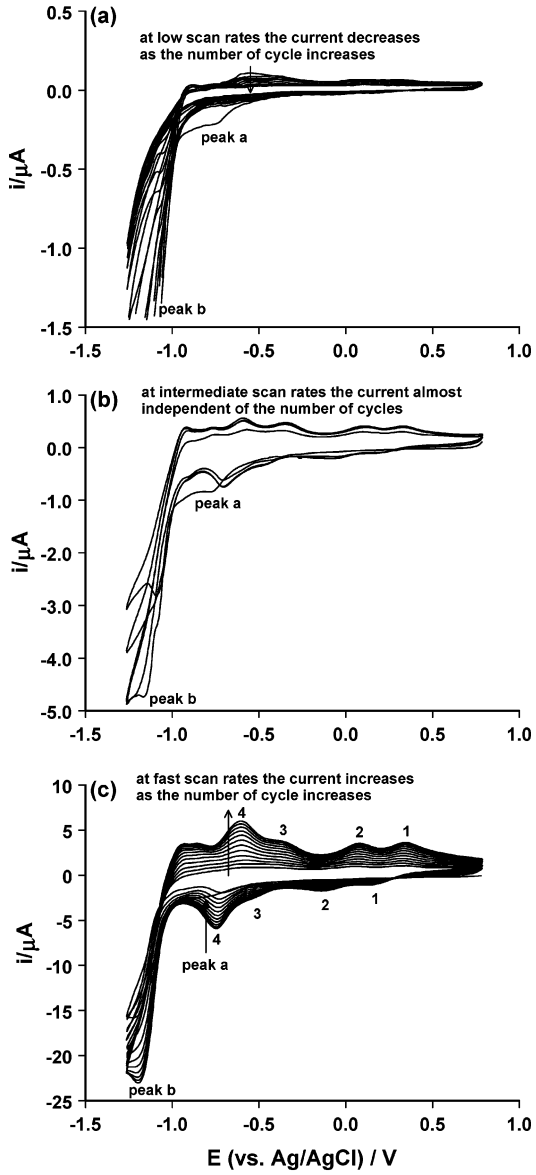

Figure 3. Scan rate dependence of the cyclic voltammetry for solid $[Bu_4N]_4[\alpha\text{-}S_2W_{18}O_{62}]$ adhered to a GC electrode (d = 1 mm) in contact with aqueous electrolyte (0.1 M Et_4NCl) at scan rates of (a) 20 (current data more negative than −1.5 μA not shown), (b) 100, and (c) 1000 mV s^{-1}.

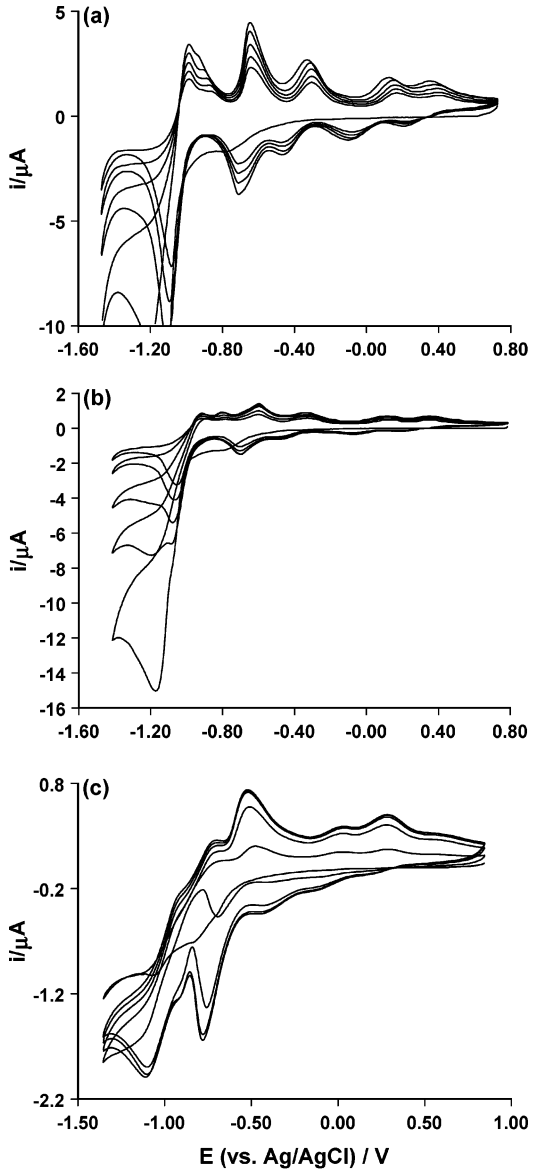

Figure 4. Cyclic voltammograms (υ = 100 mV s^{-1}) for solid $[Bu_4N]_4[\alpha\text{-}S_2W_{18}O_{62}]$ adhered to a GC electrode (d = 1 mm) in contact with electrolytes of varying Et_4NCl concentration: (a) 1 (current data more negative than −10 μA not shown), (b) 0.1, and (c) 0.01 M.

These observations are consistent with a lesser impact of product diffusion away from the electrode. Processes involving product dissolution have been simulated previously and revealed a scan rate dependence of the kind exhibited in Figure 3.[18,20,21]

The initial reduction of solid $[Bu_4N]_4[\alpha\text{-}S_2W_{18}O_{62}]$ can be assumed to require the uptake of the Et_4N^+ cation from the electrolyte to achieve charge neutralization. The current magnitude increased significantly as the concentration of Et_4NCl increased (Figure 4), consistent with this hypothesis. The importance of the electrolyte cation also is confirmed by using Bu_4NCl rather than Et_4NCl as the electrolyte (Figure S1). In this case, the Bu_4N^+ cation was common to both solid $[Bu_4N]_4[\alpha\text{-}S_2W_{18}O_{62}]$ and the electrolyte. Low currents only are detected for the solution processes, consistent with dissolution being associated with the formation of mixed cation salts of the four-electron-reduced anion $[S_2W_{18}O_{62}]^{8-}$ complex when Et_4N^+ is present in the electrolyte. Equally well-defined solution-phase voltammograms, consisting of five one-electron reduction steps with the same reversible potentials, also were obtained after the initial dissolution step when 0.1 M 1-butyl-3-methylimidazolium chloride replaced 0.1 M Et_4NCl in the aqueous electrolyte.

Equivalent studies with $[Bu_4N]_4[\gamma^*\text{-}S_2W_{18}O_{62}]$ are experimentally indistinguishable from those described above for the α isomer (compare Figures 2a and S2).

Voltammetry of Solids Adhered to a Au Working Electrode in Contact with Aqueous Electrolyte Media. The negative potential range available on a gold electrode in water at neutral pH is restricted to around −1.0 V vs Ag/

(20) Bond, A. M.; Feldberg, S. W.; Miao, W. J.; Oldham, K. B.; Raston, C. L. *J. Electroanal. Chem.* **2001**, *501*, 22.
(21) Zhang J.; Bond, A. M. *Anal. Chem.* **2003**, *75*, 2694.

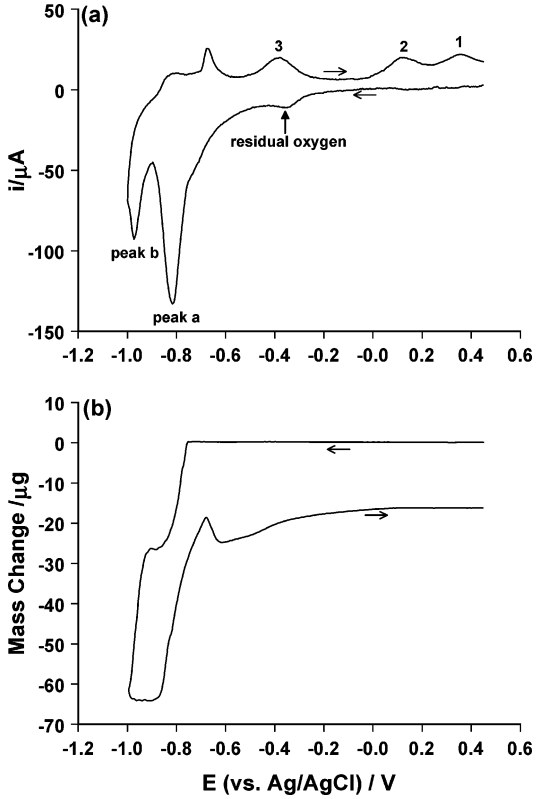

Figure 5. ECQM data ($\upsilon = 20$ mV s^{-1}) obtained for solid $[Bu_4N]_4[\alpha\text{-}S_2W_{18}O_{62}]$ adhered to a Au quartz crystal electrode in contact with aqueous electrolyte (0.1 M Et_4NCl): (a) cyclic voltammogram, (b) mass change data.

AgCl. Cyclic voltammograms obtained under these conditions with $[Bu_4N]_4[\alpha\text{-}S_2W_{18}O_{62}]$ adhered to a Au electrode ($d = 1$ mm) in contact with 0.1 M Et_4NCl are shown in Figure S3. The four solution processes 1−4 were again seen after the initial reductive scan. Estimated $E^{0'}$ values for these four processes are similar to those obtained when solid is adhered to a GC electrode (Table 1). Reversible potential data obtained with γ* are again indistinguishable from those found with the α form.

EQCM data were obtained from cyclic voltammetric experiments for $[Bu_4N]_4[\alpha\text{-}S_2W_{18}O_{62}]$ adhered to a Au quartz crystal electrode ($d = 1.32$ cm) in contact with aqueous 0.1 M Et_4NCl as the supporting electrolyte (Figure 5). Low scan rates are necessary with this much larger gold electrode to minimize the effects of uncompensated resistance. These conditions also favor enhanced dissolution.

No detectable mass change in the initial sweep in the negative potential direction was detected in EQCM experiments over the range from 0.40 to −0.74 V vs Ag/AgCl. The low current feature at about −0.3 V is attributed to reduction of residual oxygen, which is difficult to eliminate completely in the EQCM cell configuration. However, a large mass decrease is apparent as soon as the potential becomes more negative than −0.74 V, coinciding with the onset of peak a. This rapid mass loss is continuous until the potential is switched back to the positive direction at −1.00 V. A significant mass increase is observed in the range from −0.87 to −0.68 V, whereupon a small mass decrease occurs up to −0.62 V that is followed by a gradual mass increase at potentials up to 0 V. After that, no detectable mass change is apparent over the potential range from 0 to 0.40 V.

The assignment of mass changes in specified potential ranges in the above discussion is based on the assumption that the Sauerbrey equation[22] is valid under EQCM conditions at a quartz crystal gold electrode. The observed mass changes detected on this basis are consistent with the dissolution mechanism described by eqs 1−5. Zero mass change in the initial part of the scan to negative potentials is consistent with the low solubility of $[Bu_4N]_4[\alpha\text{-}S_2W_{18}O_{62}]$ in water. The initial major mass decrease after −0.74 V (Figure 5b) is attributed to the four-electron reduction of $[Bu_4N]_4[\alpha\text{-}S_2W_{18}O_{62}]$ (solid) to a water-soluble salt of $[S_2W_{18}O_{62}]^{8-}$ (peak a; Figure 5a). The second major mass decrease at −0.90 V vs Ag/AgCl appears to be associated with peak b (Figure 5a) and the apparent formation of more extensively reduced and water-soluble anions. The mass increase observed in the range from −0.85 to −0.68 V of the reverse (oxidative) potential sweep is consistent with partial reprecipitation of reduction products of lower solubility onto the electrode surface due to the relatively long time scale of the EQCM experiment ($\upsilon = 20$ mV s^{-1}). The small mass decrease observed in the range from −0.68 to −0.62 V might be associated with loss of cation Et_4N^+ from the solid phase due to oxidation of mixed cation salts. The fact that little mass change is observed at potentials more positive than −0.62 V implies that the reprecipitation of anions $[S_2W_{18}O_{62}]^{4-,5-,6-}$ is not significant, presumably for kinetic rather than thermodynamic reasons. In addition, significant quantities of material might have diffused away from the electrode.

Influence of Solvent on Reversible Potentials. The solvent dependence has been investigated for polyoxometalates by several research groups.[23,24] For example, Keita et al.[24a] found that $E^{0'}$ for the first reduction process of each $K_4[\alpha\text{-}SiW_{12}O_{40}]$ and $K_6[\alpha\text{-}P_2W_{18}O_{62}]$ depends strongly on the Lewis acidity of the solvent. More positive $E^{0'}$ values are observed in solvents with higher Lewis acidities. This observation is attributed to stabilization by the solvent of the more highly charged reduced forms, which are stronger Lewis bases compared to the corresponding oxidized form.[3,24c,25] Our data for $[S_2W_{18}O_{62}]^{4-}$ (Table 1) are consistent with this hypothesis, as potentials are more positive in H_2O, a stronger Lewis acid than CH_3CN.[14] The results in Table 1 also confirm that, whereas the presence of water is significant with respect to reversible potential values, the measured $E^{0'}$ values of both α and γ* are essentially indistinguishable in pure CH_3CN, pure H_2O, or a mixture of CH_3CN and H_2O

(22) Sauerbrey, G. *Z. Phys.* **1959**, *155*, 206.
(23) (a) Takamoto, M.; Ueda, T.; Himeno, S. *J. Electroanal. Chem.* **2002**, *521*, 132. (b) Bond, A. M.; Vu, T.; Wedd, A. G. *J. Electroanal. Chem.* **2000**, *494*, 96. (c) Himeno, S.; Takamoto, M. *J. Electroanal. Chem.* **2000**, *492*, 63. (d) Kasem, K. K. *Electrochim. Acta* **1996**, *41*, 205. (e) Itabashi, E. *Bull. Chem. Soc. Jpn.* **1987**, *60*, 1333.
(24) (a) Keita, B.; Bouaziz, D.; Nadjo, L. *J. Electrochem. Soc.* **1988**, *135*, 87. (b) Keita, B.; Nadjo, L. *J. Electroanal. Chem.* **1987**, *230*, 267. (c) Keita, B.; Nadjo, L. *J. Electroanal. Chem.* **1987**, *227*, 77. (d) Keita, B.; Nadjo, L. *J. Electroanal. Chem.* **1987**, *219*, 355. (e) Keita, B.; Nadjo, L. *J. Electroanal. Chem.* **1987**, *217*, 287. (f) Keita, B.; Nadjo, L. *J. Electroanal. Chem.* **1986**, *208*, 343.
(25) Pope, M. T.; Papaconstantinou, E. *Inorg. Chem.* **1967**, *6*, 1147.

(95:5 vol %). In addition, the results obtained in pure CH_3CN (0.1 M Bu_4NClO_4) and CH_3CN/H_2O (95:5) (0.1 M Bu_4NClO_4) media reveal that $E^{0'}$ for the first reduction process is not sensitive to the addition of 5 vol % of water. In contrast, the $E^{0'}$ values of the second and subsequent reduction processes become progressively more shifted in the positive direction. The same trend is noted in comparing data obtained in CH_3CN and H_2O where differences in the two solvents are most pronounced for process 6, which implies that the basicity of reduced forms of $[S_2W_{18}O_{62}]^{4-}$ is enhanced as the level of reduction increases.

Part B. Voltammetric Studies with α, β, and γ Isomers of $[Bu_4N]_4[SiW_{12}O_{40}]$. For the Keggin system $[SiW_{12}O_{40}]^{4-}$, α, β, and γ isomers are available.[7,8] Extensive electrochemical studies have been carried out on the α isomer in both aqueous solution and dimethylformamide (DMF).[24] Limited data are also available also on the first reduction processes of the α, β, and γ isomers in CH_3CN.[9] Unlike the $[S_2W_{18}O_{62}]^{4-}$ system, the literature data imply that the reversible potential for at least the first reduction process appears to depend significantly on the isomeric form. We now report detailed studies on the three isomers in CH_3CN (0.1 M Bu_4NClO_4) in order to quantify the isomer dependence for all processes available in this solvent.

(i) $[Bu_4N]_4[\alpha\text{-}SiW_{12}O_{40}]$. A cyclic voltammogram obtained for the reduction of $[\alpha\text{-}SiW_{12}O_{40}]^{4-}$ (5.0×10^{-4} M) in CH_3CN (0.1 M Bu_4NClO_4) at a GC electrode ($d = 3$ mm) is shown in Figure 6a. Three well-defined chemically reversible couples I−III are observed in the region from −0.8 to −2.5 V vs Fc^+/Fc with a fourth process (IV) observed but not resolved from the solvent limit.

$E^{0'}$ data for the first three processes are summarized in Table 2. Other data in Table S1 ($E^{0'}$ is independent of scan rate; $\Delta E_p \approx 55$ mV at low scan rates; I_p^{red} exhibits a linear dependence on $\upsilon^{1/2}$; $|I_p^{ox}/I_p^{red}| \approx 1$) are consistent with $[\alpha\text{-}SiW_{12}O_{40}]^{4-}$ undergoing three reversible reduction processes I−III on the voltammetric time scale, each of which involves the transfer of one electron (eq 8).

$$[\alpha\text{-}SiW_{12}O_{40}]^{4-} \xrightarrow[I]{e^-} [\alpha\text{-}SiW_{12}O_{40}]^{5-} \xrightarrow[II]{e^-} [\alpha\text{-}SiW_{12}O_{40}]^{6-} \xrightarrow[III]{e^-} [\alpha\text{-}SiW_{12}O_{40}]^{7-} \quad (8)$$

(ii) $[Bu_4N]_4[\beta\text{-}SiW_{12}O_{40}]$. Cyclic voltammograms under equivalent conditions also exhibited three well-defined redox couples I−III in the region from −0.80 to −2.4 V and a fourth reduction process (IV) near the solvent limit (Figure 6b). Thus, $[\beta\text{-}SiW_{12}O_{40}]^{4-}$ exhibits redox behavior similar to that of $[\alpha\text{-}SiW_{12}O_{40}]^{4-}$ with one fundamental difference: the reversible potential for each process is less negative by about 70 mV. A similar magnitude in potential differences also has been reported in voltammetric studies on the initial reduction steps of α and β isomers of Keggin polymolybdates, although direct comparisons with our data are not commonly possible because multiple- rather than single-electron reductions and coupled proton-transfer processes are present in the acidic media used in most of these other studies.[26]

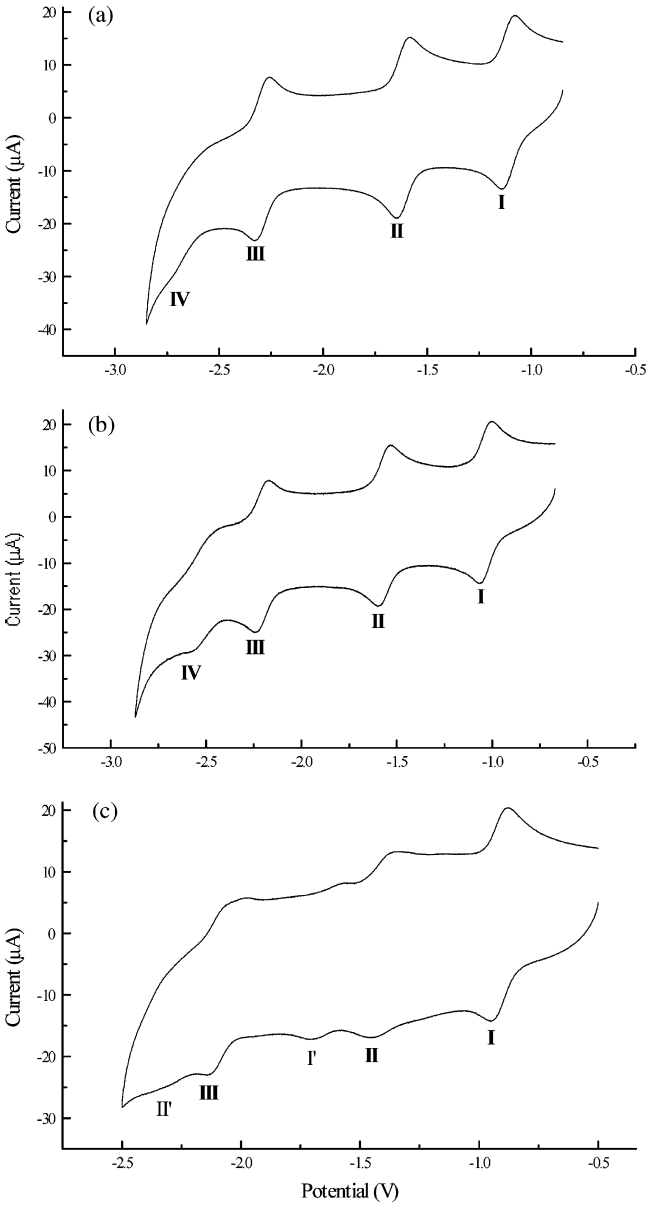

Figure 6. Cyclic voltammogram ($\upsilon = 100$ mV s^{-1}) obtained for (a) α, (b) β, and (c) γ isomers of $[SiW_{12}O_{40}]^{4-}$ (5.0×10^{-4} M) in CH_3CN (0.1 M Bu_4NClO_4).

Data obtained for the first three processes are summarized in Tables 2 and S2. The voltammetry is consistent with $[\beta\text{-}SiW_{12}O_{40}]^{4-}$ undergoing three reversible one-electron reduction processes (eq 9)

$$[\beta\text{-}SiW_{12}O_{40}]^{4-} \xrightarrow[I]{e^-} [\beta\text{-}SiW_{12}O_{40}]^{5-} \xrightarrow[II]{e^-} [\beta\text{-}SiW_{12}O_{40}]^{6-} \xrightarrow[III]{e^-} [\beta\text{-}SiW_{12}O_{40}]^{7-} \quad (9)$$

(iii) $[Bu_4N]_4[\gamma\text{-}SiW_{12}O_{40}]$. Except for the initial process I, $[\gamma\text{-}SiW_{12}O_{40}]^{4-}$ shows distinctly different voltammetry

(26) (a) Himeno, S.; Osakai, T.; Saito, A. *Bull. Chem. Soc. Jpn.* **1989**, *62*, 1335. (b) Pope, M. T. *Heteropoly and Isopoly Oxometalates*; Springer-Verlag: Berlin, 1983 and references therein.

Table 2. Reversible Potential Data[a] Obtained for the Reductions of the α, *β*, and *γ* Isomers of the Keggin System $[SiW_{12}O_{40}]^{4-}$ in Different Media

isomeric form	solvent	electrolyte	working electrode	$E^{0'}$ or E_m/V process I	process II	process III
α	CH_3CN[b]	0.1 M Bu_4NClO_4	GC	−1.110	−1.615	−2.280
β				−1.035	−1.565	−2.210
γ				−0.915	−1.390	−2.060
α	CH_3CN[c]	not stated	Hg	−0.93		
β				−0.82		
γ				−0.78		
α[d]	DMF	0.1 M $LiClO_4$	GC	−1.260		
	DMSO			−1.100		
	NMF			−0.730		
	FM			−0.545		
	H_2O	1 M $HClO_4$		−0.315		

[a] Calculated as $(E_p^{red} + E_p^{ox})/2$ from cyclic voltammograms (vs Fc^+/Fc). [b] Experimental conditions are given in the caption to Figure 6. [c] Data are from ref 9. The $E^{0'}$ value (vs SCE) has been converted to the Fc^+/Fc scale using the standard potentials of SCE and Fc/Fc^+ in aqueous phase of 0.242[19] and 0.44[33] vs NHE, respectively, with junction potential and temperature difference being neglected. Additionally, the identity of the electrolyte is unknown. Thus, although it can be concluded that the relative order of the potentials is the same as found in this study, a comparison of the absolute values is not possible. [d] Data are from ref 24a. DMF is dimethylformamide, DMSO is dimethyl sulfoxide, NMF is *N*-methylformamide, and FM is formamide.

from the α and *β* forms (Figure 6c). In this case, the term E_m is introduced to define the midpoint potential $(E_p^{red} + E_p^{ox})/2$ and to note that E_m need not be equal to $E^{0'}$ when chemical reactions are coupled to electron transfer. The E_m value, the current function $|I_p^{red}\nu^{-1/2}|$, and the current ratio $|I_p^{ox}:I_p^{red}|$ for process I were independent of scan rate within experimental error, and the magnitudes of I_p^{red} and I_p^{ox} were the same as observed for the α and *β* isomers. ΔE_p increased from 65 to 95 mV in the range $\nu = 20-1000$ mV s^{-1}. These data are consistent with an electrochemically reversible one-electron reduction for process I, affected slightly by uncompensated resistance. In this case, $E_m \approx E^{0'}$.

However, the observation of lower peak current magnitudes for all processes detected at more negative potentials than process I suggested that chemical reactions accompanied electron-transfer steps in the case of reduction of $[\gamma\text{-}SiW_{12}O_{40}]^{5-}$ to $[\gamma\text{-}SiW_{12}O_{40}]$.$^{6-}$ Data for processes, I, II, I′, and III (Figure 6c) are reported as a function of scan rate in Table S3. Parameters for process II′ are not included in Table S3, because the current magnitude is very small.

The loss of current intensity for processes II and III is attributed to the presence of chemical reactions that follow the formation of $[\gamma\text{-}SiW_{12}O_{40}]^{6-}$. Because the E_m value for process I′ for the *γ* isomer and $E^{0'}$ for process II for the α isomer have similar values (−1.64 and −1.62 V, respectively, when $\nu = 100$ mV s^{-1}), it is proposed that the two-electron-reduced species $[\gamma\text{-}SiW_{12}O_{40}]^{6-}$ undergoes isomerization to $[\alpha\text{-}SiW_{12}O_{40}]^{6-}$, which is then immediately oxidized to $[\alpha\text{-}SiW_{12}O_{40}]^{5-}$, with both species then undergoing further one-electron reduction process at different potentials (process II, eq 8, and process I′, eq 10). The potential of process II for the *γ* isomer (−1.4 V) does not correspond with the potential of any processes detected for the α and *β* isomers. Consequently, its E_m value is associated with the $[\gamma\text{-}SiW_{12}O_{40}]^{5-/6-}$ couple. For similar reasons, the process at −2.1 V for the *γ* isomer is associated with the $[\gamma\text{-}SiW_{12}O_{40}]^{6-/7-}$ couple (eq 10). Process II′ has a small current magnitude (Figure 6c), but its E_m value of about −2.3 V matches that of process III for the α isomer (eq 10). Overall, the results obtained suggest that the two-electron-reduced anion $[\gamma\text{-}SiW_{12}O_{40}]^{6-}$ undergoes isomerization to $[\alpha\text{-}SiW_{12}O_{40}]^{6-}$ to give a complex reduction scheme of the kind presented in eq 10

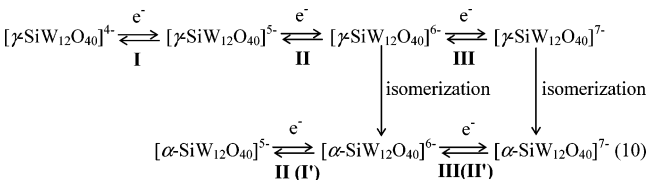

$E^{0'}$ data obtained in this and other studies are summarized in Table 2. In accordance with the findings of other workers,[9] we confirm that $[\gamma\text{-}SiW_{12}O_{40}]^{4-}$ is more easily reduced than the α and *β* isomers in CH_3CN. However, in our more extensive data set, we now find that the two-electron-reduced $[\gamma\text{-}SiW_{12}O_{40}]^{6-}$ undergoes isomerization to $[\alpha\text{-}SiW_{12}O_{40}]^{6-}$ (eq 10) on the voltammetric time scale. Although transformations between the α and *β* forms of Keggin polyoxometalates in different redox levels has been well documented,[1a,g,26−28] *γ* → α isomerization of $[\gamma\text{-}SiW_{12}O_{40}]^{6-}$ on the voltammetric time scale has not previously been reported. However, *γ**-to-α transformation is associated with the one-electron bulk electrolysis of $[\gamma^*\text{-}S_2W_{18}O_{62}]^{4-}$.[5]

Part C. Possible Origins of Differences in the Isomeric Dependence of Reversible Potentials of Keggin and Dawson Polyoxometalates. In contrast to the experimentally indistinguishable reversible potentials found for reduction of α and *γ** isomers of the Dawson anion $[S_2W_{18}O_{62}]^{4-}$ in both solution and solid phases, clear differences are detected for the α, *β*, and *γ* isomers of the Keggin anion $[SiW_{12}O_{40}]^{4-}$. The charge distribution in polyoxometalate compounds and its influence on the redox chemistry of polyoxometalates have been a topic of wide interest[26b,29,30] This distinct difference in the dependence of $E^{0'}$ values on isomeric form might be related to the different charge densities and charge distributions of the overall 4− charged anions and their more negatively charged reduced forms.

(27) Chiang M.; Dzielawa, J. A.; Dietz, M. L.; Antonio, M. R. *J. Electroanal. Chem.* **2004**, *567*, 77.
(28) López, X.; Maestre, J. M.; Bo, C. Poblet, J. M. *J. Am. Chem. Soc.* **2001**, *123*, 9571.
(29) (a) Coronado, E.; Gómez-Garcia, C. J. *Chem. Rev.* **1998**, *98*, 273. (b) Pope, M. T. In *Mixed Valence Compounds*; Brown, D. B., Ed.; Reidel Publishing Co.: Dordrecht, The Netherlands, 1980 and references therein.
(30) (a) López, X.; Bo, C.; Poblet, J. M.; Sarasa, J. P. *Inorg. Chem.* **2003**, *42*, 2634. (b) Suaud, N.; Gaita-Ariño, A.; Clemente-Juan, J. M.; Sanchez-Marin, J.; Coronado, E. *J. Am. Chem. Soc.* **2002**, *124*, 15134. (c) Neiwert, W. A.; Cowan, J. J.; Hardcastle, K. I.; Hill, C. L.; Weinstock, I. A. *Inorg. Chem.* **2002**, *41*, 6950. (d) Juraja, S.; Vu, T.; Richardt, P. J. S.; Bond, A. M.; Cardwell, T. J.; Cashion, J. D.; Fallon, G. D.; Lazarev, G.; Moubaraki, B.; Murray, K. S.; Wedd, A. G. *Inorg. Chem.* **2002**, *41*, 1072. (e) Maestre, J. M.; López, X.; Bo, C.; Poblet, J. M.; Casañ-Pastor, N. *J. Am. Chem. Soc.* **2001**, *123*, 3749. (f) Keita, B.; Lu, Y. W.; Nadjo, L.; Contant, R. *Eur. J. Inorg. Chem.* **2000**, 2463. (g) Duclusaud, H.; Borshch, S. A. *Inorg. Chem.* **1999**, *38*, 3489. (h) Neier, R.; Trojanowski, C.; Mattes, R. *J. Chem. Soc., Dalton Trans.* **1995**, 2521. (i) Nieves, C.; Baker, L. C. W. *J. Am. Chem. Soc.* **1992**, *114*, 10384. (j) King, R. B. *Inorg. Chem.* **1991**, *30*, 4437. (k) Sanchez, C.; Livage, J.; Launay, J. P.; Fourier, M. *J. Am. Chem. Soc.* **1983**, *105*, 6817.

Table 3. Reversible Potentials (V vs SCE) Reported for the Reduction of $[As_2W_{18}O_{62}]^{6-}$ and $[P_2W_{18}O_{62}]^{6-}$ in Aqueous Electrolyte Media (0.9 M NaCl/0.1 M HCl) at a Rotating Carbon Rod Electrode[a]

	$E^{0'}$ or E_m/V		
isomeric form	$[As_2W_{18}O_{62}]^{6-/7-}$	$[As_2W_{18}O_{62}]^{7-/8-}$	$[As_2W_{18}O_{62}]^{8-/10-}$
$[\alpha\text{-}As_2W_{18}O_{62}]^{6-}$	0.09	−0.09	−0.38
$[\beta\text{-}As_2W_{18}O_{62}]^{6-}$	0.12	−0.06	−0.35
$[\gamma\text{-}As_2W_{18}O_{62}]^{6-}$	0.15	−0.03	−0.33
$[\gamma^*\text{-}As_2W_{18}O_{62}]^{6-}$	0.12	−0.06	−0.35
α-, β-, γ-$[P_2W_{18}O_{62}]^{6-}$	*b*	*b*	*b*

[a] Data are taken from ref 4. [b] $E^{0'}$ values are shifted by ca. −0.04 V relative to those of the corresponding $[As_2W_{18}O_{62}]^{6-}$ anion.

Experimental evidence from NMR and ESR studies suggests that, upon reduction, the electrons are added to the 12 belt atoms of 18 total W atoms present in the α Dawson structure.[30j,31] Given that the belt regions of the α and γ* isomeric forms are not too dissimilar, as suggested by theoretical studies on isomers of $[P_2M_{18}O_{62}]^{n-}$ (M = W and Mo) and $[P_2W_{15}V_3O_{62}]^{n-}$,[30a] then the thermodynamics associated with their reduction processes can be expected to be similar (including the strength of ion pairing that should contribute to $E^{0'}$ values for these highly charged anions). Thus, the reason why $E^{0'}$ values for the reduction of $[S_2W_{18}O_{62}]^{4-}$ do not exhibit a significant α, γ* isomeric dependence might be associated with the fact that connectivity and charge density differences in their belt regions are small.

The smaller Keggin $[SiW_{12}O_{40}]^{4-}$ anion clearly has a higher charge density than the Dawson $[S_2W_{18}O_{62}]^{4-}$ structure. In the case of $[\alpha\text{-}XM_{12}O_{40}]^{n-}$ anions, all electrons are delocalized over all equivalent M atoms.[32] In contrast, upon reduction of $[\beta\text{-}XM_{12}O_{40}]^{n-}$ anions, the added electrons are constrained to the six MO_6 octahedra adjacent to the rotated M_3O_{13} group.[1a] Moreover, in the case of $\gamma\text{-}XM_{12}O_{40}{}^{n-}$, which contains four types of nonequivalent M atoms, the electron added to these systems prefer to stay on 4 of the 12 M atoms.[9] Therefore, the 12 W atoms in the α-, β-, and γ-$[SiW_{12}O_{40}]^{4-}$ isomeric forms are expected to differ significantly in their relative forms of connectivity and hence charge distribution. Thus, the basicity of the reduced forms and ion paring capacity and hence $E^{0'}$ values might be expected to more strongly isomer dependent, as found experimentally.

Literature $E^{0'}$ data available for the α, β, γ, and γ* isomers of $[As_2W_{18}O_{62}]^{6-}$ and $[P_2W_{18}O_{62}]^{6-}$ Dawson systems are summarized in Table 3.[4] Comparisons with data obtained in this study for 4− charged polyoxometalates reveal two significant features. First, $E^{0'}$ values for α and γ* isomers of the 6− charged $[X_2W_{18}O_{62}]^{6-}$ (X = As, P) exhibit a larger isomeric dependence than found for the lower 4− charged $[S_2W_{18}O_{62}]^{4-}$ system, which presumably reflects the importance of a higher charge density. Second, the α, β, γ, and γ* isomeric $E^{0'}$ dependence for the Dawson $[X_2W_{18}O_{62}]^{6-}$ structures is significantly less than that for the α-, β-, and γ-$[SiW_{12}O_{40}]^{4-}$ Keggin forms. Larger connectivity differences in the Keggin case are assumed to contribute to this difference, with the contribution from charge density being less clear-cut in this particular comparison because both size and charge are larger in the $[X_2W_{18}O_{62}]^{6-}$ structures. All available data therefore imply that both connectivity and charge density play important roles in the magnitude of isomeric differences of reversible potentials observed in Dawson and Keggin polyoxometalate anions.

Rationalization of the absolute $E^{0'}$ order is still to be achieved. It has been confirmed in this work that the reversible potentials for reduction of $[\beta\text{-}SiW_{12}O_{40}]^{4-}$ are less negative than those for $[\alpha\text{-}SiW_{12}O_{40}]^{4-}$. Analogous α/β potential differences of around 100 mV also have been reported in voltammetric studies in acidic media on the initial reduction steps of α and β isomers of Keggin polymolybdates,[26] e.g., $[XMo_{12}O_{40}]^{4-}$ (X = Si or Ge) and $[YMo_{12}O_{40}]^{3-}$ (Y = P or As), and in ionic liquids for the reduction of $[\alpha\text{-}PW_{12}O_{40}]^{3-}$. However, the order of ease of reduction within a group of isomers can change with extent of reduction[26] and is not readily predicted solely on the basis of connectivity and charge distribution differences. Theoretical studies[28] predict that β isomers should be easier to reduce than α forms for Keggin structures. However, these calculations do not take into account solution-phase ion pairing, and no theoretical calculations appear to be available to rationalize the experimental observation that the Keggin γ isomer is even easier to reduce than the α and β forms. More extensive theoretical studies of highly charged polyoxometalate anions, including solution-phase ion pairing terms, are needed to provide rationalizations of difference in the absolute values of $E^{0'}$ as a function of redox level and structure.

Acknowledgment. The authors thank the Australian Research Council and the Monash University Research Fund for financial support of this project.

Supporting Information Available: Additional Figures S1−S3 containing cyclic voltammograms for the reduction of solid $[Bu_4N]_4[\alpha\text{-}S_2W_{18}O_{62}]$ (Figure S1), $[Bu_4N]_4[\gamma^*\text{-}S_2W_{18}O_{62}]$ (Figure S2) at a GC electrode, and $[Bu_4N]_4[\alpha\text{-}S_2W_{18}O_{62}]$ (Figure S3) at a Au electrode in contact with aqueous electrolyte media and cyclic voltammetric data for α-, β-, and γ-$[SiW_{12}O_{40}]^{4-}$ in CH_3CN (0.1 M Bu_4NClO_4) at a GC macrodisc electrode (Tables S1−S3). This material is available available free of charge via the Internet at http://pubs.acs.org.

IC049043X

(31) See, for example: Kozik, M.; Hammer, C. F.; Baker, L. C. W. *J. Am. Chem. Soc.* **1986**, *108*, 2748.
(32) See, for example: Acerete, R.; Hammer, C. F.; Baker, L. C. W. *J. Am. Chem. Soc.* **1982**, *104*, 5384.
(33) Bard, A. J.; Fan, F. R.-F.; Mirkin, M. V. In *Electroanalytical Chemistry*; Bard, A. J., Ed.; Marcel Dekker: New York, 1994; Vol. 18, p 243.
(34) Izutsu, K. *Electrochemistry in Nonaqueous Solutions*; Wiley: New York, 2002.